

The QCD string tension curve, the ferromagnetic magnetization, and the quark-antiquark confining potential at finite Temperature

P. Bicudo*

CFTP, Departamento de Física, Instituto Superior Técnico, Av. Rovisco Pais, 1049-001 Lisboa, Portugal

We study the string tension as a function of temperature, fitting the SU(3) lattice QCD finite temperature free energy potentials computed by the Bielefeld group. We compare the string tension points with order parameter curves of ferromagnets, superconductors or string models, all related to confinement. We also compare the SU(3) string tension with the one of SU(2) Lattice QCD. With the curve providing the best fit to the finite temperature string tensions, the spontaneous magnetization curve, we then show how to include finite temperature, in the state of the art confining and chiral invariant quark models.

I. INTRODUCTION

Motivated by the discovery of the Quark-Gluon Plasma at the CMS at CERN, and RHIC at BNL laboratories and by the future experiments at RHIC-II, LHC and FAIR, quark model computations are presently addressing with more and more detail chiral symmetry breaking and deconfinement at finite temperature or finite density. Here we show how to upgrade the confining quark-antiquark potential, with a string tension σ function of the temperature T .

In the 80's a new quark model, the Chiral Quark Model (χ QM), was developed [1–3], including not only the quark confining potential of the early quark models, but also the spontaneous breaking of chiral symmetry of the Nambu and Jona-Lasinio model. Although the χ QM can only be approximately derived from QCD in the Coulomb gauge hamiltonian formalism, although it has not yet been fully calibrated to the finest details of the hadronic spectrum, and although Lorentz invariance is only present in the kinetic energy, it is nevertheless the only QCD inspired model able to explicitly include both quark confinement and quark-antiquark vacuum condensation. Thus the χ QM is the most comprehensive QCD model, adequate to study any possible system of quarks, gluons, or hadrons, and to provide, at least, a qualitative answer to the questions one may ask to QCD.

So far the χ QM studies of chiral symmetry breaking at finite temperature or density have assumed a temperature independent string tension, *i. e.* the same confining potential at all temperatures, since the work of Yaouanc, Oliver, Pène, Raynal, Jarfi and Lazrak [4]. Within this approximation, many studies of chiral symmetry have found that chiral symmetry breaking is maintained at all temperatures. The first calculations at finite temperature or at finite density are already 20 years old [4, 5], but presently finite temperature or finite density are interesting many authors, including the São Paulo group [6, 7], the Graz group [8], the Pittsburgh group [9] and others. Only Lo and Swanson using ring diagrams, *i.*

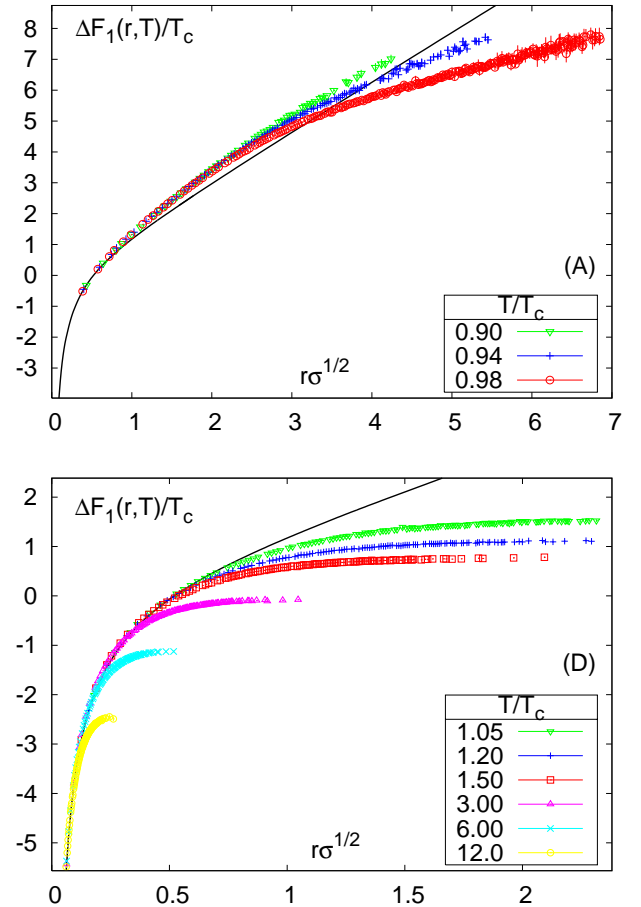


FIG. 1: We show examples finite temperature static quark-antiquark potentials, in particular the $T < T_c$ and $T > T_c$ Lattice QCD data for the free energy F_1 , thanks to [10–14]Olaf Kaczmarek et al. The solid line represents the $T = 0$ static quark-antiquark potential. In this paper we discuss the use of the free energy as a finite temperature quark-antiquark potential.

e. quark loops beyond the ladder approximation, has been able to find chiral symmetry restoration at a finite critical temperature T_c , since the quark loops effectively affect the confining potential.

*Electronic address: bicudo@ist.utl.pt

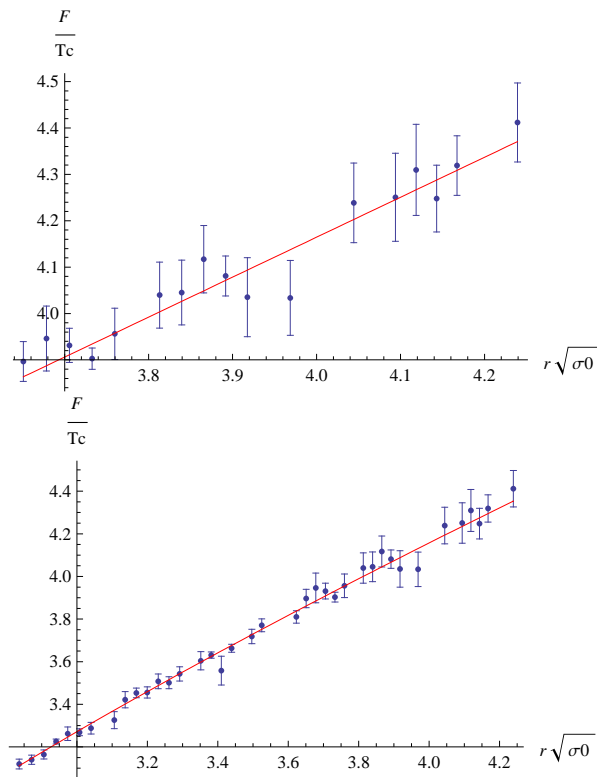


FIG. 2: Fits of the Bielefeld's group free energy at $T < T_c$, here in the case of $T = 0.90T_c$, in the top we use a linear fit and in the bottom we use a linear + coulomb fit. We cut the low distance, or infrared, part of the lattice data shown in Fig. 1, in such a way that the fit is independent as possible on the cutoff. Similar cuts and fits are applied for the other temperatures.

Nevertheless the finite temperature static quark-antiquark free and internal energies at some finite temperatures T have already been computed in SU(3) lattice QCD, by the Bielefeld group [10–14], and they are available to be included in the χ QM. In particular, the first part of the quark-antiquark potential to suffer finite temperature effects is the long distance confining part. In what concerns the short range Coulomb part of the quark-antiquark potential, it survives up to any temperature. Moreover the short-range Coulomb potential is included in the ultraviolet renormalization program of QCD, thus it is relevant for the quark mass renormalization, but can be neglected for chiral symmetry breaking [15]. While the Coulomb potential at finite temperature is quite relevant for the heavy quarkonia, since even slightly above the deconfinement critical temperature T_c the J/ψ and η_c remain bound [16, 17], for the binding of light quarks the confining part of the quark-antiquark potential, parametrized by the linear string tension, is crucial.

Moreover, although the Polyakov loop is presently the preferred order parameter for deconfinement [18, 19], other order parameters may be used, [20, 21] and in par-

T/T_c	σ	IR cutoff	χ^2/dof
0.00	1.545 ± 0.002	1.0	-
0.90	0.861 ± 0.072	3.6	0.52
0.94	0.587 ± 0.028	4.3	1.96
0.98	0.429 ± 0.005	4.1	0.22
1.00	0.00 ± 0.000	-	-

TABLE I: Fits of the string tension in units of $T_c^{-1}\sigma(0)^{-1/2}$ for the longer distance part of the Kaczmarek *et al* lattice data, using the ansatz $F(r) = c + \sigma r$.

ticular the string tension is a possible order parameter for the deconfinement phase transition.

Thus here we specialize in the finite temperature string tension [22], and show how to include the results of finite T Lattice QCD in the χ QM, including finite T in the string tension of the confining part of the quark-antiquark potential. This work continues the study of the SU(3) string tension, computed for the first time by the Bielefeld Group, [22].

In Section II we fit the SU(3) string tension from the long distance part of the recent static quark-antiquark free energy from the lattice QCD results of the Bielefeld Group, and we compare the SU(3) string tension with the SU(2) string tension. In section III we compare the string tensions with the order parameter curves of ferromagnets, superconductors or string models, all related to confinement, and find that the curve closer to the SU(3) string tension is the magnetization curve. In Section IV we use the curve inspired in the magnetization of ferromagnets, to also compute the entropy string tension, the internal energy string tension, and to estimate the finite T string tension of the quark-antiquark potential. In Section V, we conclude.

II. FITTING THE SU(3) AND SU(2) LATTICE QCD FINITE T STRING TENSIONS WITH DIFFERENT ANSATZE

This work continues the study of the SU(3) string tension, computed for the first time by the Bielefeld Group, [22], in a seminal paper also discussing in detail the finite temperature phenomenology. In this 2000 paper, the Bielefeld group computes the string tension below T_c utilizing colour averaged (over the colour singlet and colour octet) Polyakov loops, to extract colour averaged free energies. The results then obtained confirmed a 1st order phase transition for the deconfinement phase transition, as expected for SU(3) since the string tension was found to remain finite at $T < T_c$, while it is vanishing at $T > T_c$, with a small discontinuity at $T = T_c$.

More recently, the Bielefeld group computed free energies for the colour singlet quark-antiquark static system, utilizing gauge fixing. Here we fit the string tension of these free energies, [10–14] recently computed by Doring, Hubner, Kaczmarek, Karsch, Vogt and Zantow in SU(3)

T/T_c	σ	α	IR cutoff	χ^2/dof
0.00	1.395 ± 0.005	1	0.3	-
0.90	0.667 ± 0.012	10	2.8	0.51
0.94	0.515 ± 0.008	11	2.8	1.56
0.98	0.287 ± 0.002	14	3.0	0.21
1.00	0.00 ± 0.000	-	-	-

TABLE II: Fits of the string tension in units of $T_c^{-1}\sigma(0)^{-1/2}$ for the longer distance part of the Kaczmarek *et al* lattice data, using the ansatz $F(r) = c - \alpha \frac{\pi}{12r} + \sigma r$.

Lattice QCD by , for $T < T_c$, see Fig. 1. For $T > T_c$ the fit is trivial since the confinement potential, and the string tension, vanish. To extract the string tension as a function of the temperature $\sigma(T)$ we try different ansatz to fit the free energy, and we cut the low distance part with an infrared cutoff. We choose the lowest possible cutoff, in the region where our fit is stable for changes of the cutoff. We also check that our fit is not too far from the of $\chi/\text{dof} \simeq 1$. As different ansatz to fit the long distance part of the potential, we use a constant and a linear term,

$$F(r) = c(T) + \sigma(T)r \quad (1)$$

or a constant, a coulomb and a linear terms

$$F(r) = c(T) - \frac{\alpha(T)}{r} + \sigma(T)r \quad (2)$$

or, as in the SU(3) Bielefeld fit [22] and in the similar SU(2) fit of reference [23], a constant, a linear and a Logarithmic terms

$$F(r) = c(T) - a(T) \log(r) + \sigma(T)r \quad (3)$$

and in all of them we check the stability of the string tension. We apply these ansatz to the free energies at the different temperatures, and this is illustrated if Fig. 2 for the case of $T = 0.90T_c$. It occurs that the fit with a Logarithmic term of Eq. (3) is not sufficiently stable, in the sense that whenever we increase the infrared cutoff, the string tension σ change, and thus we abandon this ansatz. The other two fits of Eqs. (1) and (2) are stable, in the sense that a distance r_{cut} can be used as an infrared cutoff, and that if we increase this infrared cutoff distance, the string tension is essentially unchanged.

The details on the fits are show in Tables I and II. The simpler constant plus linear fit of of Eq. (1) needs a higher cutoff r_{cut} than the constant plus linear plus Coulomb fit of eq. (3). The two different sets of string tensions are depicted in Fig. 3. Notice that to the finite temperatures of $T = 0.90T_c$, $T = 0.94T_c$, and $T = 0.98T_c$ we add the cases of $T = 0$ with the string tension $\sigma(0)$ and of $T > T_c$ with a vanishing string tension $\sigma(T) = 0$.

It occurs however that the string tensions computed with the two different ansatz of Eqs. (1) and (2) differ, even when they are normalized to $\frac{\sigma(T)}{\sigma(0)}$. Notice that

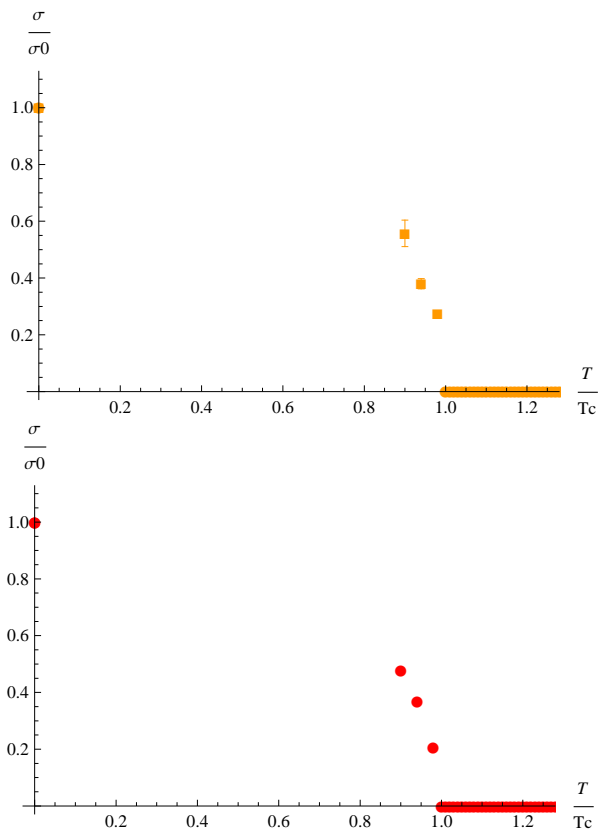


FIG. 3: The results of the fits, present in Table I (top) and in Table II (bottom) , can be summarized in a dimensionless curve of $\sigma(T)/\sigma(0)$ as a function of T/T_c . The bottom fit, of a constant plus a Coulomb plus a linear term has a greater stability that the simpler top fit, and smaller error bars.

the $T = 0$ potential has the Luscher term $\frac{\pi}{12r}$ and the same term is expected to also exist at finite temperature, the ansatz including a Coulomb term of Eq. (2) has a broader stability for changes of the infrared cutoff r_{cut} , and produces points with a smoother alignment. Thus of all our fits of the string tension of the Bielefeld free energies, the ansatz of Eq. (2), with the fits of Table II and Fig. 3 (bottom) appears to be the best.

In Fig. 4 we plot our fits, present in Table I and in Table II, together with the string tensions σ that were fitted by the Bielefeld Group in 2000 [22]. They are all consistent, with our linear fit slightly larger than the Bielefeld fits in the year 2000, and with our linear plus Coulomb fit only slightly lower than the Bielefeld fit. In Fig. 5 we also compare the SU(3) string tension critical curve (bullets) with the SU(2) string tension critical curve (squares) of reference [23]. The SU(2) string tension is smaller than the SU(3) one, and it corresponds to a larger critical exponent than the critical exponent of SU(3).

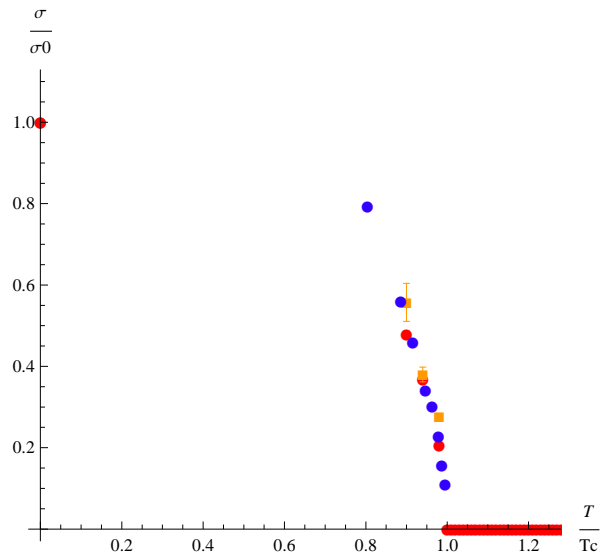


FIG. 4: The results of the fits, present in Table I and in Table II, together with the SU(3) fits in the year 2000 of the Bielefeld Group [22], summarized in a dimensionless curve of $\sigma(T)/\sigma(0)$ as a function of T/T_c .

III. FERROMAGNETIC, SUPERCONDUCTOR AND STRING INSPIRED ANSATZE FOR THE QCD STRING TENSION CURVE

The string tension σ is crucial for the spontaneous breaking of chiral symmetry, and for the light hadron spectra. Thus it is important to know the string tension $\sigma(T)$ at all temperatures, starting from $T = 0$ and not just at temperatures of the order of T_c . Since in Section II the string tension was only computed for a few temperatures, close to T_c , we now compare the string tension to similar other curves or order parameters, with the aim to propose an ansatz for $\sigma(T)$.

We remark that we expect for QCD a 1st order phase transition with a discontinuity at $T = T_c$, but with only a weak discontinuity. Thus we may use as ansatz for the string tension curve, in the case where we are interested in all the interval $T \in [0, T_c]$ and not just in a narrow neighbourhood of T_c , second order parameter curves. Indeed the points in Fig. 3 are close to second order, or continuous phase transition, with a critical exponent in the order parameter. Notice that we do not claim here that the transition is not the expected 1st order one, we are simply concerned with the fit of the potential to be used in the quark model.

To find an ansatz for the string tension curve we first study order parameter curves of physical systems related to confinement. The Ising model not only is a model of ferromagnetism, but it is also a model of confinement, and in particular the critical exponent of the SU(2) string tension is similar to the three-dimensional Ising model exponent. Another model of confinement is the dual superconductor model, since the colour electric flux tubes

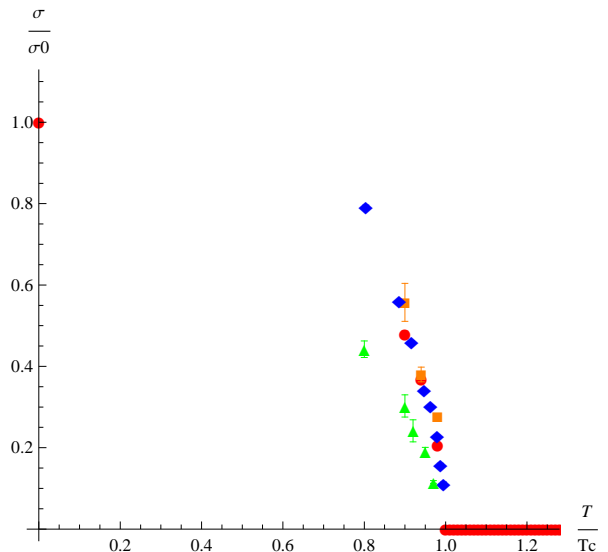


FIG. 5: Comparing the SU(3) string tension critical curve (bullets, squares and diamonds) of Fig. 4, with the SU(2) string tension critical curve (triangles) of Ref. [23]. The critical curve of SU(2) is flatter, and it corresponds to a larger critical exponent 0.63 than the critical exponent $\simeq 0.5$ of SU(3).

existing between confined quarks and antiquarks are confined as vortices in superconductors. And colour electric flux tube confinement can be approximated, in the limit of thin flux tubes, by string models. Thus we may inspire ourselves in ferromagnetic materials, in the Ising model, in superconductors either in the BCS model or in the Ginzburg-Landau model, or in string models, to suggest ansatz for the string tension curve.

We order the different ansatz used in these related systems, from the simpler to define, to the more sophisticated one. The coherence length of a Ginsburg-Landau superconductor [24] is,

$$\frac{\xi}{\xi_0} = \sqrt{1 - \frac{T}{T_c}} \quad (4)$$

the string tension of a finite T string [25], extrapolated from $T \simeq T_c$ to $T \simeq 0$, is,

$$\frac{\sigma}{\sigma_0} = \sqrt{1 - \left(\frac{T}{T_c}\right)^2} \quad (5)$$

the empirical fit to the penetration length of a superconductor [26] is,

$$\frac{\lambda}{\lambda_0} = \sqrt{1 - \left(\frac{T}{T_c}\right)^4} \quad (6)$$

the spontaneous magnetization of a ferromagnet [27] is the solution of the algebraic equation,

$$\frac{M}{M_{sat}} = \tanh\left(\frac{T_c}{T} \frac{M}{M_{sat}}\right), \quad (7)$$

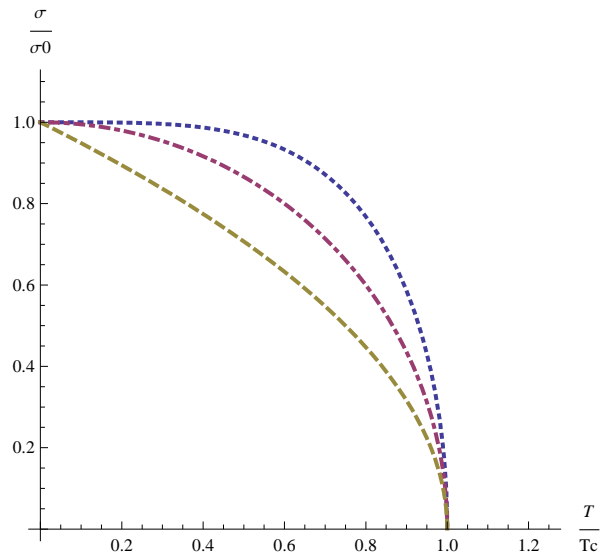


FIG. 6: We show the string tension curves $\frac{\sigma}{\sigma(0)}$ as a function of $\frac{T}{T_c}$ of the parametric ansatze of Eq. (4) in a dashed line, Eq. (5) in a dot-dashed line, and Eq. (6) in a dotted line. The solution of Eq. (8) for a large Debye frequency w_D is similar to the dashed line.

and the mass gap of a BCS superconductor [26] is a solution of the integral equation,

$$1 = gN(0) \int_0^{w_D} \frac{dw}{w^2 + \Delta^2} \tanh \frac{(w^2 + \Delta^2)^{1/2}}{2T}. \quad (8)$$

We compare the curves of Eqs. (4), (5), (6) in Fig. 6, and we show how to plot the curve of Eq. (7) in Fig. 7. The mass gap solution of Eq. (8) is not unique since it depends on two parameters, the density of states $gN(0)$ and the Debye frequency w_D . In the limit of a very small w_D , Eq. (8) is equivalent to Eq. (7). The opposite limit $w_D \gg gN(0)$ occurs in real type I superconductors [26], in which case the curve $\Delta(T)$, in dimensionless units, is quite similar to the circular curve of Eq. (5). Thus we do not plot the solution of Eq. (8) in a separate curve.

In Fig. 8 we plot the Magnetization, solution of Eq. (7), together with the string tensions σ that fitted from SU(3) Lattice QCD data. The solution of Eq. (7) provides our best fit of the string SU(3) tensions. We also show in Fig. 8 our second best ansatz, the one of the empirical penetration length of a ferromagnet in eq. (6). In Fig. 9 we also compare the magnetization curve with the SU(3) string tension critical curve computed in Ref. [22], and with the fit

$$\frac{\sigma}{\sigma(0)} = 1.21 \sqrt{1 - 0.990 \left(\frac{T}{T_c}\right)^2} \quad (9)$$

used in Ref. [22] to measure the finite string tension at T_c as an evidence for a 1st order phase transition. Both the fit of Eq. (9), similar to Eq. (5) but with a different norm

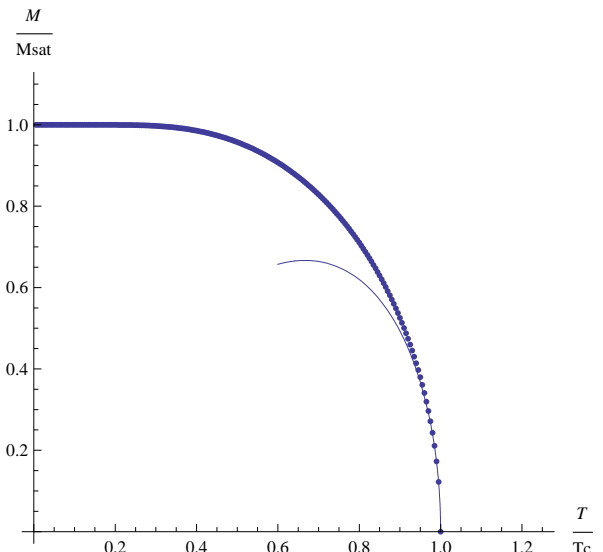


FIG. 7: The critical curve for $\frac{M}{M_{sat}}$ as a function of $\frac{T}{T_c}$ is shown in a dotted solid line (one dot per each of our numerical fixed point solution). We find the critical curve solving Eq. (7) with the fixed point method. The solution is essentially a flat constant curve for low T but for $T \simeq T_c$ it behaves like the square root as in eq. (11), also depicted here.

and with a small temperature shift of $10^{-2}T_c$, showing evidence for the 1st order phase transition, and the SU(3) string are quite close to our magnetization curve for T close to T_c . But the magnetization curve is the only one that extends up to the correct solution at $T = 0$. The magnetization curve is as close to our string tension curve as it is close to the magnetization of a real ferromagnet.

Since the magnetization curve fits so well the SU(3) string tensions, we now briefly review how it is derived. The ferromagnetic spontaneous magnetization curve as a function of temperature is a text book curve, detailed for instance in the *Feynman Lectures on Physics* [27]. Let us briefly review the simplest case, with spins in the $\frac{1}{2}$ representation. Then, in a magnetic field B , each spin has only two possible states with energies, $\pm\mu_0 B$ where $\mu_0 = \frac{g}{2} \frac{e\hbar}{2m}$ is not the chemical potential but it is the magnetic moment of a quantum spin. This leads to the magnetization,

$$M = N\mu_0 \tanh \frac{\mu_0 B}{kT}. \quad (10)$$

The case that interests is the case of a ferromagnet, when there is no external field, and the magnetic mean field affecting the spin is proportional to the magnetization M . $N\mu_0$ is the saturation magnetization M_{sat} . We then get the algebraic Eq. (7) equation for the magnetization curve,

$$\frac{M}{M_{sat}} = \tanh \left(\frac{T_c}{T} \frac{M}{M_{sat}} \right),$$

the Eq. providing the best ansatz for our string tension curve.

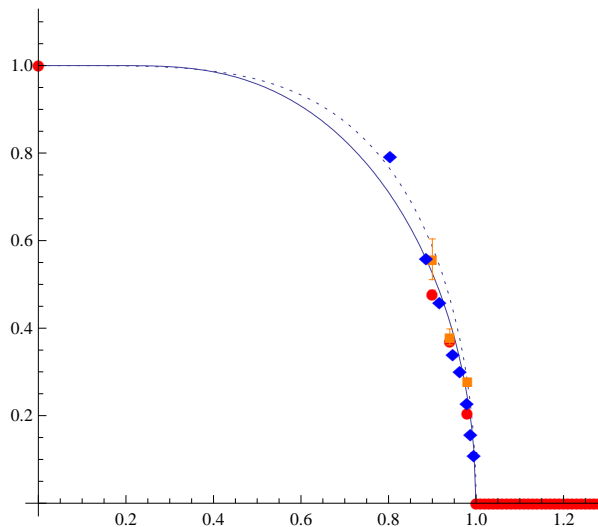


FIG. 8: Comparing the ferromagnet magnetization M/M_{sat} critical curve (solid line) of Fig. 7 with the SU(3) string tension $\sigma/\sigma(0)$ (bullets, squares and diamonds) of Fig. 2, both as a function of $T \simeq T_c$. In this plot, M/M_{sat} is quite close to $\sigma/\sigma(0)$. We also show (dotted line) the empirical curve of Eq. (6) which provides the second best fit of all the ones we tried.

To analyze the curve solution to Eq. (7), we start by getting the extreme points of the curve solution to eq. (7), noticing that $\tanh \infty = 1$, thus when $T = 0$ we get $\frac{M}{M_{sat}} = 1$. Also when the only solution of $x = \tanh x$ is $x = 0$ thus when $T = T_c$ we have $\frac{M}{M_{sat}} = 0$ as expected. Moreover, expanding the hyperbolic tangent close to $T \simeq T_c$, we get ,

$$\begin{aligned} \frac{M}{M_{sat}} &\simeq \frac{T_c}{T} \frac{M}{M_{sat}} - \frac{1}{3} \left(\frac{T_c}{T} \frac{M}{M_{sat}} \right)^3 \\ \Rightarrow \frac{M}{M_{sat}} &\simeq \sqrt{3 \frac{T}{T_c} \left(\frac{T}{T_c} - 1 \right)}. \end{aligned} \quad (11)$$

This shows that in this case the critical exponent for the magnetization M is $\frac{1}{2}$. This corresponds to a second phase transition since the magnetization is the first derivative of the free energy with regards to the chemical potential. For a complete solution of Eq. (7), we use the fixed point method, with 10^4 iterations for each temperature T . In Fig. 7 we show the solution of Eq. (7) obtained with the fixed point expansion, and also the approximate solution shown in of Eq. (11) for $T \simeq T_c$.

It is striking that the curve $\frac{M(T/T_c)}{M_{sat}}$, which is derived from a simple two-state quantum spin system, not only fits the magnetization curve of many ferromagnets, but also fits essentially the string tension curve of finite temperature quenched SU(3) QCD. Possibly this occurs since confinement can also be partially understood in the simplest two-state Ising Model. In particular Dıgal, Fortunato and Petreczky [23] computed the string tension of quenched SU(2), also with fits of the free energy, and

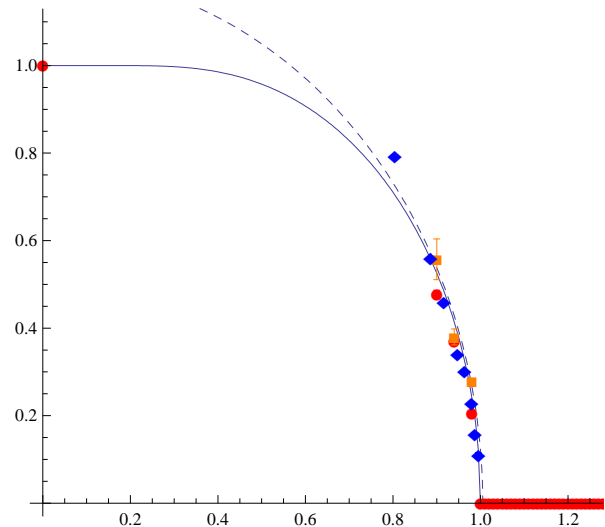


FIG. 9: Comparing the magnetization curve (solid line) with the SU(3) string tension critical curve (bullets) computed in Ref. [22]. We also show (dashed line) the fit $1.21(1 - 0.990(T/T_c)^2)^{1/2}$ used in Ref. [22] to measure the finite string tension at T_c as an evidence for a 1st order phase transition.

found that the SU(2) string tension has the same critical exponent 0.63 of the 3-dimensional Ising model. Thus in Fig. 5 we also compare the SU(3) string tension critical curve (bullets) with the SU(2) string tension critical curve (squares) of reference [23]. The critical curve of SU(2) is lower than the SU(3) curve, and it corresponds to a slightly larger critical exponent than the critical exponent $\simeq 0.5$ of SU(3), obtained when neglecting the first order discontinuity at $T = T_c$. Nevertheless the similarity between our SU(3) string tension and the the SU(2) and Ising model string tensions suggests that the SU(3) confinement is relatively simple. Indeed Lattice QCD is able to simulate comprehensively hadronic physics using a relatively small number of 100 to 1000 configurations, and this is only possible if SU(3) confinement has relatively few degrees of freedom. It may also be relevant for the understanding of SU(3) confinement, that the mean field model of ferromagnetism provides a better fit to the SU(3) string tension curve than the Ising spin-spin interaction model. Also, when comparing with a the circular curve of Eq. (5), the SU(3) string tension curve is flatter at the origin, and thus closer to the curve of Eq. (6), while the SU(2) string tension curve is steeper and thus closer to the curve of Eq. (4).

Thus, based on our numerical results, and also confident in the relative simplicity of SU(3) QCD confinement, and on the small discontinuity of the string tension $\sigma(T)$ at T_c we may use, in what concerns finite temperature quark models, as an ansatz for the string tension,

$$\sigma(T/T_c) \simeq \sigma(0) \frac{M(T/T_c)}{M_{sat}}. \quad (12)$$

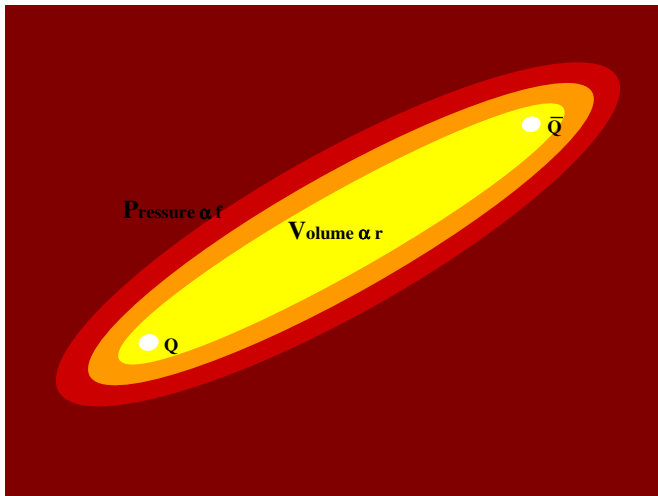


FIG. 10: A free illustration of a static flux tube, where we compare the force f to the pressure P , and the length r to the volume V .

IV. THE FREE ENERGY, THE INTERNAL ENERGY, AND THE FINITE TEMPERATURE QUARK-ANTIQUARK CONFINING POTENTIAL

In the χ QM, the potential energy V is used in the mass gap equation to compute the quark constituent mass and chiral symmetry breaking, and in the Salpeter equation to compute the hadron spectrum. However, in Lattice QCD, first the quark-antiquark free energy F is computed from the pair of Polyakov loops P ,

$$\text{Tr} \{P(0)P^\dagger(r)\} = C \exp\left(\frac{-F}{kT}\right), \quad (13)$$

and it is the free energy of the a static quark-antiquark pair that we have studied in Sections II and III. The potential energy of the quark-antiquark pair is related to the quark-antiquark force,

$$dV = -f dr \quad (14)$$

where a linear flux tube is assumed as in Fig. 10, and we can study the thermodynamics of the flux tube using the equivalence $f dr = p dV$ for the work of the quark-antiquark pair. Then we get the usual thermodynamic relations, relevant at finite T , for the free energy F ,

$$F(r) = -f dr S dT, \quad (15)$$

and for the internal energy E ,

$$E(r) = -f dr + T dS. \quad (16)$$

The quark potential V is identical to the free energy F in a reversible isothermal transformation with $dT = 0$,

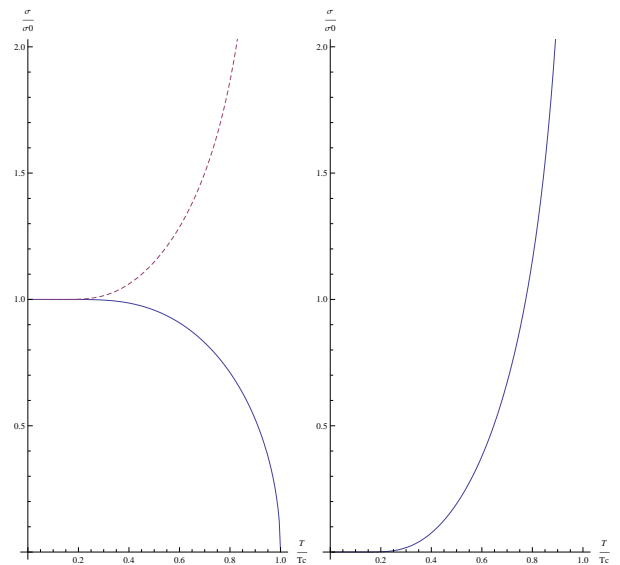


FIG. 11: Free energy (solid line) compared with the internal energy (dashed line) (left), entropy divergent at $T = T_c$ (right).

and is identical to the internal energy E in a reversible adiabatic transformation with $TdS = 0$.

Since we have a good ansatz for the confining part of F , *i. e.* for the string tension, determined in Section III, we may compute the string tension of the entropy S ,

$$S = -\frac{\partial F}{\partial T}, \quad (17)$$

and then also compute the string tension of the internal energy,

$$E = F + TS. \quad (18)$$

In Fig. 11, we compare the different string tensions. Notice that the entropy diverges when $T \rightarrow T_c$, and this is well known from the computations of the Bielefeld Group at temperatures close to T_c . In particular the divergence is,

$$\sigma_S \rightarrow \frac{\sigma_0}{2T_c} \sqrt{\frac{3}{\frac{T}{T_c} - 1}}, \quad (19)$$

and thus the internal energy E also diverges when $T \rightarrow T_c$, this is clear in Fig. 11.

Now, in a hadron, or in the vacuum, it is not totally clear what energy, either F or E to use as a the quark-antiquark potential. A main assumption of the χ QM, and of any quark model, is that the static quark-antiquark computed in Lattice QCD can be also be used, at least qualitatively, for light quarks. One assumes that the quark moves relatively slowly compared to the flux tube formation typical scale, and that the gluonic flux tube adapts to the quark and antiquark positions. This is an adiabatic assumption, in the quantum mechanical

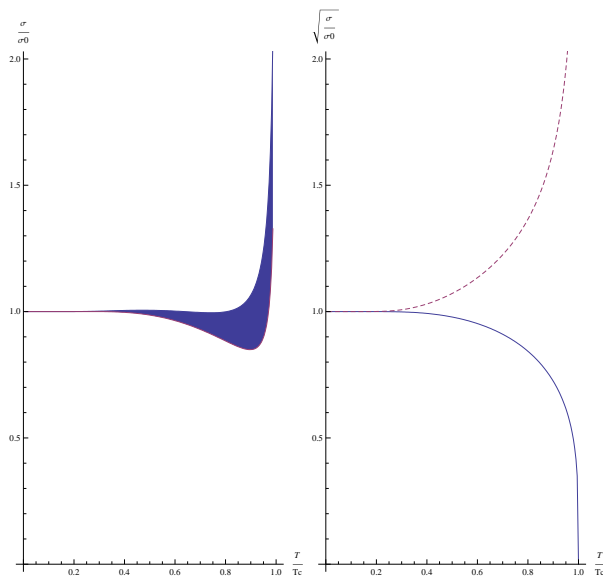


FIG. 12: Flattening the potential combining some internal energy to the free energy (left), flattening the free (solid line) and internal (dashed line) energies with a square root (right).

sense and not in the thermodynamic sense. Thus with the mechanical adiabatic assumption of a slow motion of the flux tube, the quark movement is sufficiently slow in the heat bath of the hot medium at temperature T , and we can assume that the flux tube transformation is isothermal. Then the potential energy is well approximated by the free energy $V \simeq F$. Nevertheless, possibly the quarks move too fast for a completely isothermal transformation of the flux tube, and then the flux tube transformation may have a small contribution from the internal energy E , identical to the potential energy when no heat is exchanged with the heat bath, in that case,

$$V = (1 - \omega)F + \omega E, \quad (20)$$

where ω should be a small number. In that case the potential dependence in the temperature T is flatter for $T < T_c$. In particular we also depict in Fig. 12 the cases where $0.1 < \omega < 0.3$ where the string tension is nearly flat up to close to $T = T_c$.

Notice however that there is an evidence contrary to the use of the internal energy E for light quarks. The problem with the internal energy is not only its divergence at $T = T_c$, but also that it is larger than the free energy, $E > F$. Yamamoto, Suganuma and Iida found in Lattice QCD that the presence of light quark does reduce the string tension [28]. Thus, presently, the best model for the string tension at finite T remains the one of Eqs. (7) and (12).

V. CONCLUSION

We fit the finite temperature string tension from the free energies of a quark-antiquark pair computed in SU(3) lattice QCD by the Bielefeld group [10–14]. We find a good ansatz for the string tension at all temperatures, the magnetization curve of a ferromagnet. While evidence for a 1st order phase transition exists [22], the difference to the 2nd order magnetization curve is small, and therefore the magnetization curve is a good ansatz for the quark-antiquark potential at finite temperature, adequate to be included in the χ QM.

We find that a constant string tension may also be arguably used at $T < T_c$. Thus at $T < T_c$ the quark model computations present in the literature are acceptable. The main arguments are that the free energy F string tension is already relatively flat up to T close to T_c and that the light hadron spectrum scales with $\sqrt{\sigma}$ which is flatter than the string tension, as in Fig. 12. Moreover, if a contribution from the internal energy E string tension can be justified, then the string tension is further flattened up to T close to T_c . And the 1st order discontinuity, although small, also flattens the string tension.

However, at $T > T_c$ the string tension vanishes, and in this sense the χ QM calculations present in the literature must be corrected. To encompass all temperatures, the free energy string tension of Eqs. (7) and (12) should be used in the χ QM, or at least a step function with a transition at T_c could be approximately used.

Nevertheless, the relative instability of the fits of the finite temperature string tension, and the importance of the finite T Coulomb or logarithmic potentials suggest that eventually the finite T χ QM will have to go beyond the simple use of a long range linear potential, including also medium range and short range potentials [15, 29].

In what concerns the Lattice QCD studies of the free energy at finite temperature, it would be interesting if more results would be further computed. In particular the subtle 1st order SU(3) discontinuity at $T = T_c$ [22], deserves more detailed studies in the region of $T \simeq T_c$. Moreover at smaller temperatures, $T \in]0, 0.8T_c[$ there is no Lattice QCD data. Thus we anticipate that the research of finite T quark-antiquark potentials will remain very interesting in the future.

Acknowledgments

I thank Olaf Kaczmarek for sharing his SU(3) Lattice QCD data on the free energy, the internal energies and the free energy string tensions, Peter Petreczky for sharing his SU(2) Lattice QCD Data on the free energy string tension, and Nuno Cardoso for his codes on linear and non-linear fits. I am grateful to Marlene Nahrgang, to Olaf Kaczmarek, to Pedro Sacramento, to Jan Pawlowski and to Fabien Buis-

seret for discussions on the QCD phase diagram motivating this paper. I acknowledge the financial support

of the FCT grants CFTP, CERN/FP/109327/2009 and CERN/FP/109307/2009.

-
- [1] A. Le Yaouanc, L. Oliver, S. Ono, O. Pene and J. C. Raynal, Phys. Rev. D **31**, 137 (1985); A. Amer, A. Le Yaouanc, L. Oliver, O. Pene and J. C. Raynal, Phys. Rev. Lett. **50**, 87 (1983); A. Le Yaouanc, L. Oliver, O. Pene and J. C. Raynal, Phys. Rev. D **29**, 1233 (1984);
- [2] S. L. Adler and A. C. Davis, Nucl. Phys. B **244**, 469 (1984).
- [3] P. Bicudo and J. E. Ribeiro, Phys. Rev. D **42**, 1611 (1990); Phys. Rev. D **42**, 1625; Phys. Rev. D **42**, 1635.
- [4] A. Le Yaouanc, L. Oliver, O. Pène, J. C. Raynal, M. Jarfi and O. Lazrak, Phys. Rev. D **37**, 3691 (1988); A. Le Yaouanc, L. Oliver, O. Pène, J. C. Raynal, M. Jarfi and O. Lazrak, Phys. Rev. D **37**, 3702 (1988); A. Le Yaouanc, L. Oliver, O. Pène, J. C. Raynal, M. Jarfi and O. Lazrak, Phys. Rev. D **38**, 3256 (1988).
- [5] P. Bicudo, Phys. Rev. Lett. **72**, 1600 (1994).
- [6] O. A. Battistel and G. Krein, Mod. Phys. Lett. A **18**, 2255 (2003).
- [7] S. M. Antunes, G. Krein, V. E. Vizcarra and P. K. Panda, Braz. J. Phys. **35**, 877 (2005).
- [8] L. Y. Glozman and R. F. Wagenbrunn, Phys. Rev. D **77**, 054027 (2008) [arXiv:0709.3080 [hep-ph]].
- [9] P. M. Lo and E. S. Swanson, arXiv:0908.4099 [hep-ph].
- [10] M. Doring, K. Hubner, O. Kaczmarek and F. Karsch, Phys. Rev. D **75**, 054504 (2007) [arXiv:hep-lat/0702009].
- [11] K. Hubner, F. Karsch, O. Kaczmarek and O. Vogt, arXiv:0710.5147 [hep-lat].
- [12] O. Kaczmarek and F. Zantow, Phys. Rev. D **71**, 114510 (2005) [arXiv:hep-lat/0503017].
- [13] O. Kaczmarek and F. Zantow, arXiv:hep-lat/0506019.
- [14] O. Kaczmarek and F. Zantow, PoS **LAT2005**, 192 (2006) [arXiv:hep-lat/0510094].
- [15] P. Bicudo, Phys. Rev. D **79**, 094030 (2009) [arXiv:0811.0407 [hep-ph]].
- [16] P. Bicudo, M. Cardoso, P. Santos and J. Seixas, arXiv:0804.4225 [hep-ph].
- [17] P. Bicudo, J. Seixas and M. Cardoso, arXiv:0906.2676 [hep-ph].
- [18] L. D. McLerran and B. Svetitsky, Phys. Lett. B **98**, 195 (1981).
- [19] L. D. McLerran and B. Svetitsky, Phys. Rev. D **24**, 450 (1981).
- [20] F. Zantow, O. Kaczmarek, F. Karsch and P. Petreczky, Nucl. Phys. Proc. Suppl. **106**, 519 (2002) [arXiv:hep-lat/0110103].
- [21] F. Zantow, O. Kaczmarek, F. Karsch and P. Petreczky, arXiv:hep-lat/0110106.
- [22] O. Kaczmarek, F. Karsch, E. Laermann and M. Lutgemeier, Phys. Rev. D **62**, 034021 (2000) [arXiv:hep-lat/9908010].
- [23] S. Digal, S. Fortunato and P. Petreczky, Phys. Rev. D **68**, 034008 (2003) [arXiv:hep-lat/0304017].
- [24] P. de Gennes, "Superconductivity of Metals and Alloys", published by Addison Wesley Publishing Company, Reading, Massachusetts, ISBN 0-201-51007-3 (1966).
- [25] M. Gao, Phys. Rev. D **40**, 2708 (1989).
- [26] A. Fetter, J. Walecka, "Quantum Theory of Many-Particle Systems", published by Dover Publications, Mineola, New York, ISBN 0-486-42827-3 (1971).
- [27] R. Feynman, R. Leighton, M. Sands, "The Feynman Lectures on Physics", Vol II, chap. 36 "Ferromagnetism", published by Addison Wesley Publishing Company, Reading, Massachusetts, ISBN 0-201-02117-x (1964).
- [28] A. Yamamoto, H. Suganuma and H. Iida, Phys. Lett. B **664**, 129 (2008) [arXiv:0708.3610 [hep-lat]].
- [29] P. J. A. Bicudo and A. V. Nefediev, Phys. Rev. D **68** (2003) 065021 [arXiv:hep-ph/0307302].